Combustion synthesis of mechanically activated powders in the Nb–Si system

Filippo Maglia, Chiara Milanese, and Umberto Anselmi-Tamburini[a)]
Department of Physical Chemistry and C.S.T.E./CNR, University of Pavia, V. le Taramelli 16, I-27100 Pavia, Italy

Stefania Doppiu and Giorgio Cocco
Department of Chemistry, Via Vienna 2, I-07100 Sassari, Italy

(Received 28 January 2002; accepted 13 May 2002)

The effect of the mechanical activation of the reactants on the self-propagating high-temperature synthesis (SHS) of niobium silicides was investigated. SHS experiments were performed on reactant powder blends of composition Nb:Si = 1:2 and Nb:Si = 5:3 pretreated for selected milling times. A self-sustaining reaction could be initiated when a sufficiently long milling time was employed. At short milling times, the reactions self-extinguished or propagated in an unsteady mode. Combustion peak temperature, wave velocity, and product composition were markedly influenced by the length of the milling treatment. Single-phase products could be obtained for sufficiently long milling times. Observation of microstructural evolution in quenched reactions together with isothermal experiments allowed clarification of the mechanism of the combustion process and the role played by the mechanical activation of the reactants.

I. INTRODUCTION

The excellent thermal and mechanical properties of niobium silicides have resulted in them being considered for high-temperature applications. For example, $NbSi_2$ has been considered as a potential substitute for superalloys in high-temperature structural applications, as it has one of the highest melting points among the silicides and a density less than that of nickel-based superalloys.[1] Nb_5Si_3/Nb has been reported to show excellent thermochemical stability and resistance to coarsening up to 1500 °C,[2,3] together with high bond strength and high fracture toughness at room temperature.[4,5] Due to their high melting points, the synthesis of niobium silicides has been attempted using nonconventional techniques, including mechanical alloying (MA),[6,7] self-propagating high-temperature synthesis (SHS),[8] and field-activated combustion synthesis (FACS).[9,10] Mechanical alloying allows pure $NbSi_2$ to be obtained from the elements. The process, however, is not characterized by the gradual transition from reactants to products typical of mechanical alloying: a fast, spontaneous, combustion-like phenomena occur after few hours of milling and drives within few seconds to the final product. Surprisingly, the synthesis through SHS resulted to be quite problematic. Despite the fairly high adiabatic temperatures (1879 K for $NbSi_2$ and 2513 K for Nb_5Si_3), it has been necessary to preheat the reacting mixtures at temperatures between 523 and 723 K to obtain a self-propagating reaction. Furthermore, for both stoichiometries the final product contained multiple phases. For the Nb:Si = 1:2 mixture $NbSi_2$ and Si were identified, and for the Nb:Si = 5:3 mixture $NbSi_2$, α–Nb_5Si_3, β–Nb_5Si_3, and Nb were identified. Using the FACS method Gedevanishvily and Munir[9] were able to produce a self-propagating reaction in the Nb:Si = 5:3 mixture imposing fields above a threshold value of 7.4 V/cm. The mode of wave propagation and the composition of the products depended largely on the magnitude of the applied field. At low fields pulsating propagation was observed and the product was multiphase, while at higher fields the combustion was steady and the product contained only the low and high temperature modification of Nb_5Si_3. On the other hand, FACS was ineffective in the synthesis of $NbSi_2$ because the mixture Nb:Si = 1:2 shows a very low electrical conductivity.

Recently, it has been reported that combustion reactions that are thermodynamically or kinetically hindered can be activated if preceded by mechanical treatments of the reactants through prolonged milling, a process referred to as mechanically activated SHS or MASHS.[11–13] Mechanical activation of the reactants, in fact, has been

[a)]Address all correspondence to this author.
e-mail: tau@chifis.unipv.it

shown to be able to influence the macrokinetic characteristics (reaction temperatures and propagation rates) of the combustion reaction.[14] Intensive or prolonged milling, however, results in some systems in a spontaneous ignition of the reacting mixture.[15–20] This process has been referred to as mechanically induced self-propagating reaction, or MSR.[21]

The aim of this work is to further our understanding of the fundamental aspects of the mechanical activated SHS process as applied to the synthesis of intermetallic compounds in the binary system Nb–Si.

The binary system Nb–Si contains three intermetallic compounds: $NbSi_2$, Nb_5Si_3, Nb_3Si.[22] Nb_5Si_3 has been reported to exist in three different crystallographic forms, a tetragonal, low-temperature form (α–Nb_5Si_3) and a hexagonal, high temperature form (β–Nb_5Si_3), with a transition temperature lying between 1900 and 2100 °C. A second tetragonal, carbon-stabilized form was also reported. The heats of formation as well as the calculated adiabatic combustion temperatures of formation from the elements, T_{ad}, are reported in Table I.[9,22]

II. EXPERIMENTAL MATERIALS AND METHODS

Appropriate amounts of niobium and silicon powders were milled in a hardened steel vial using a Spex Mixer-Mill (Spex Certiprep, Metuchen, NJ) (model 8000) equipped with a 230 V–15 Hz motor operating at 1425 rpm, corresponding (in its standard configuration) to 875 cycles/min of the vial. One hardened steel grinding ball of 13.7 g and 1.5 cm in diameter and constant powder batches of 8 g were used. Milling runs were carried out in continuous mode. The vial temperature was continuously monitored during milling runs with a thin lamella-shaped Pt-resistance thermometer fixed on the external side of the vial. Samples were prepared using −325 mesh (<45 μm) silicon powder of 99.5% purity and −325 mesh niobium powder of 99.8% purity supplied by Alfa (Karlsruhe, Germany). Powder handling and milling were done under an atmosphere of highly purified argon in a glovebox. The levels of the residual humidity, oxygen, and nitrogen are controlled to the ppm level. More details concerning powder treatment are reported elsewhere.[23] We just note that an impact energy of approximately 0.1 J/hit was used, corresponding to a reduced milling intensity of about 0.4 W/g.

TABLE I. Crystal structures, enthalpies of formation, and adiabatic combustion temperatures for the silicides of niobium.

Compounds	Crystal structure	$\Delta H_{f,298}$ (kJ/mol of atoms)[16]	T_{ad} (K), T_0 = 298
$NbSi_2$	$P6_222$	−46.0	1879
α–Nb_5Si_3	$I4/mcm$	−60.7	2513
β–Nb_5Si_3	$P6_3/mcm$	−60.7	2513
C-Nb_5Si_3[a]	$I4/mcm$	−60.7	2513

[a]Tetragonal metastable form. Stabilized by the presence of small amounts of C, O, and N.

After milling, powders were cold-pressed to form cylindrical pellets 8 mm in diameter and 10 mm in height. The pellets were then ignited inside a stainless steel reactor by using an electrically heated tungsten coil placed 1–2 mm away from the top of the sample. To ensure identical ignition condition in all the experiments and to reduce the ignition time and sample preheating, 0.5 g of thermite mixture ($Zr + Fe_2O_3$) was pressed above the reacting pellet. The thermite mixture ignites almost instantaneously and in most cases favors the formation of a flat and even reaction front inside the Nb–Si mixture. All experiments were performed in a high-purity argon (99.998%) atmosphere. Temperature profiles were measured with a two-color pyrometer, with a resolution time of 0.01 s, focused on the middle of the sample, while the propagation rates were determined from video recordings of the reaction front.

Structural and microstructural characterization of reactants and products were made by optical microscopy, scanning electron microscopy (SEM), an energy dispersion electron microprobe (EDS), and powder x-ray diffraction (XRPD). A Zeiss Axioplan optical microscope (Oberkochen, Germany) and a Cambridge SEM Stereoscan 200 (Cambridge, United Kingdom) operated at 30 kV and equipped with a back-scattered electron detector and a Link microprobe were used. XRPD analysis was performed using a diffractometer Philips 1710 (Eindhoven, The Netherlands) equipped with a copper anode (operated at 40 kV and 35 mA), graphite-curved monochromator on the diffracted beam, and a proportional counter.

Bulk diffusion couples were prepared using circular wafers of Nb and Si with a diameter of 5 mm and a thickness of 1–2 mm. Prior to assembly, the mating surfaces were prepared by polishing first with silicon carbide abrasive paper and then with 1-μm diamond paste and finally rinsed with acetone. The cleaned Nb and Si wafers were then pressed tightly together between spring loaded alumina rods inside an alumina tube, and the resulting assembly was placed in a furnace under a high-purity argon flux (99.998%). The diffusion couples were held at temperatures ranging from 1200 to 1350 °C for times ranging from 2 to 16 h. The temperature was measured with a thermocouple in contact with a thin alumina layer (1 mm) placed behind the Si slice. After cooling, the samples were embedded in epoxy resin, sectioned, polished, and examined by optical and electron microscopy. The composition of the reacted zone was determined by EDS.

Interactions between Nb solid and Si liquid were studied by immersion tests performed in isothermal conditions at temperatures ranging between 1450 and 1600 °C

for times ranging between 2 and 16 min. A 0.65-g amount of Si powders was melted in an alumina crucible (10 mm in diameter), under a pure argon atmosphere, inside a graphite resistance furnace. The temperature was measured with a thermocouple in contact with the bottom surface of the crucible. The Nb sample, in the form of a 2.5-mm rod, was attached to a sample holder fixed at the top of the furnace, its long axis parallel to the crucible axis. Once the desired temperature was attained, the Nb sample was dipped into the molten Si. At the end of the reaction time, the system was air-quenched by quickly pushing the crucible outside the hot zone of the furnace. More details about the experimental setup are reported elsewhere.[24]

III. RESULTS

A. Mechanically activated self-propagating high-temperature synthesis (MASHS)

MASHS experiments were performed on samples with stoichiometries corresponding to Nb:Si = 1:2 and Nb:Si = 5:3. Both compositions undergo spontaneous combustion during the milling process. The occurrence of the mechanically induced self-propagating reaction is observed well before the appearance of any product phase in the milled powders. The corresponding milling times (hereafter t_{ig}) resulted to be equal to approximately 553 min for the Nb:Si = 1:2 composition and approximately 295 min for the Nb:Si = 5:3 composition.

Upon milling, the powder morphology changed considerably. An example of these modifications is shown in Fig. 1. At the beginning of the milling process [Fig. 1(a)], the reactant powders appear as irregular particles several micrometers in diameter. Upon milling the evolution of the microstructure appears to be controlled by the elastic and mechanical properties of the reactants [Figs. 1(b) and 1(c)]. The ductile Nb is, in fact, promptly deformed to give lamellar particles [Fig. 1(b)], while the brittleness of silicon leads to a refinement of particles mainly by fracture processes. The fine Si particles result to be packed between the metallic Nb lamellae. At longer milling times the lamellae width is reduced to a value of few micrometers and the mixture appears more homogeneous when observed at low magnification [Fig. 1(c)]. The milled mixture appears in the form of round shaped agglomerates of diameter up to several hundreds of micrometers made of tightly packed reactants. The dimensions of the coherent diffraction domains, $\langle L_{hkl} \rangle$, which express the subgrain sizes, and the corresponding strain content, $\langle \epsilon \rangle$, of niobium and silicon in the course of the alloying process were assessed from the line profile analysis of the x-ray diffraction patterns by resorting to Rietveld refinement methods. Data are collected in Table II as a function of the milling time. $\langle L_{hkl} \rangle$ for silicon, decreasing by almost 1 order of magnitude, highlights its higher brittleness, as it is also apparent from the distinguishing $\langle \epsilon \rangle$ trend.

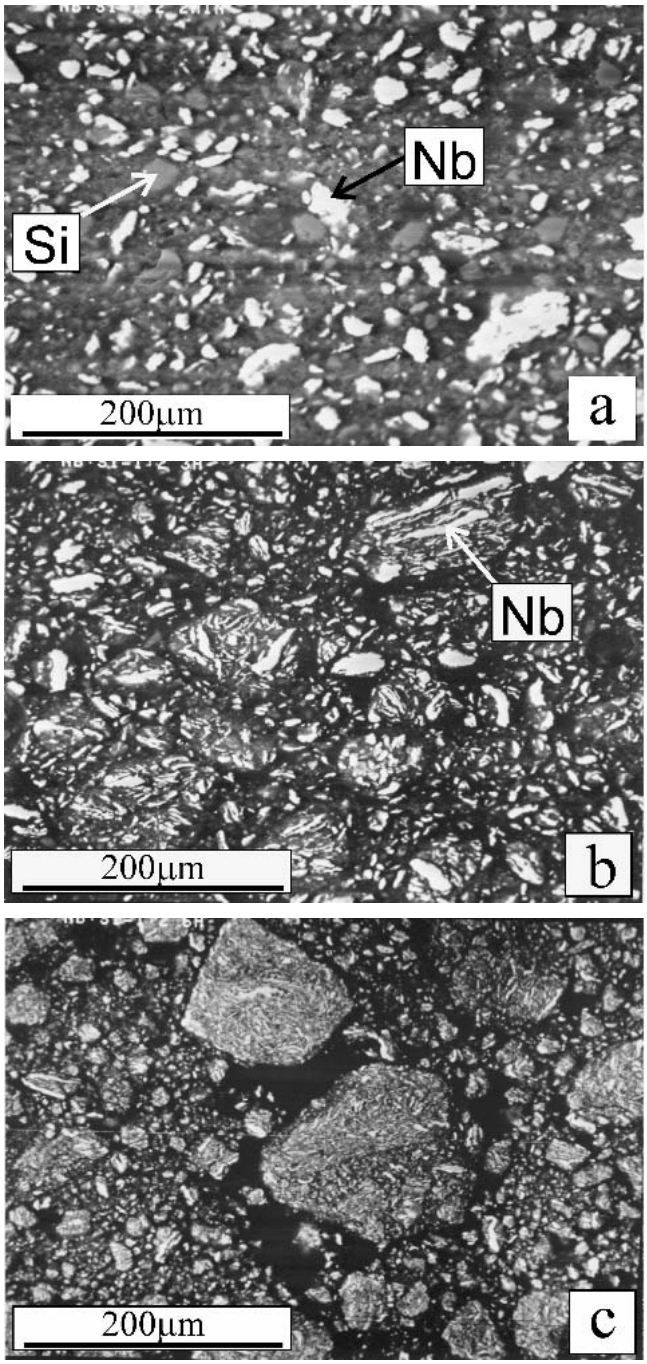

FIG. 1. Scanning electron micrographs of Nb:Si = 1:2 powder particles undergoing ball milling: (a) after 60 min of milling; (b) after 180 min of milling; (c) after 540 min of milling. The SEM backscattered image is on the polished section.

The SHS experiments were performed on samples which underwent increasing milling periods up to the self-ignition time. The macrokinetic characteristics of the combustion process (combustion mode, temperature profile, and propagation rate) were found to be largely dependent on the extent of the milling time for both compositions (Figs. 2 and 3). When unmilled powders of

composition Nb:Si = 1:2 were employed, a pulsed front that self-extinguished before reaching the opposite end of the sample was observed. The measured peak temperature was intermediate between the Si (1414 °C) and the Si-rich eutectic melting point (1385 °C).[22] When pretreated powders were employed, the Nb:Si = 1:2 blends produced stable, stationary fronts whose peak temperature and propagation rates increased monotonically with milling time.

Similar results were found for the composition Nb:Si = 5:3 (Fig. 3). In this case, the ignition of unmilled powders is even more difficult and the front extinction occurs almost immediately, when the front moves outside the zone heated by the ignition coil. Unstable propagation (either pulsating or spin mode) was observed for milling times up to 120 min. However, when powders milled for longer times are used, the propagation of the combustion front becomes stationary. Also for this composition, an increase in peak combustion temperature and propagation rates was observed as a function of milling time (hereafter m.t.). It must be noticed however that, at long milling times, the peak temperature stabilizes at a value around 1900 °C, while at m.t. = 80 min the temperature is just above the Si melting point. Also for this composition the front velocity increases more than 1 order of magnitude as an effect of ball-milling treatments.

For both compositions not only the peak temperature but also the shape of the entire temperature profile was dependent on m.t. Figures 4 and 5 show the temperature profiles recorded during the front propagation, with the pyrometer spot focused on the middle portion of the sample. As the leading edge of the combustion front enters

TABLE II. Effect of milling on lattice parameters, crystallite size, and strain.

Milling time (min)	a_{Nb}	$\langle L_{hkl}\rangle_{Nb}$ (nm)	ϵ_{Nb}	a_{Si}	$\langle L_{hkl}\rangle_{Si}$ (nm)	ϵ_{Si}
		Nb:Si = 1:2				
0	3.299	42 ± 4	0.0017	5.424	136 ± 14	3E – 5
60	3.302	19 ± 2	0.0063	5.427	45 ± 4	1.0E – 4
180	3.302	18 ± 2	0.0075	5.428	31 ± 3	1.1E – 4
360	3.303	17 ± 2	0.0077	5.429	20 ± 2	1.5E – 4
540	3.306	13 ± 1	0.0081	5.431	11 ± 1	3.3E – 4
		Nb:Si = 5:3				
2	3.300	53 ± 5	8E – 4	5.426	112 ± 11	4E – 5
80	3.301	18 ± 2	0.0063	5.426	45 ± 4	1.0E – 4
120	3.302	17 ± 2	0.0065	5.426	28 ± 3	1.6E – 4
240	3.302	15 ± 1	0.0061	5.424	12 ± 1	9.5E – 4
285	3.303	11 ± 1	0.0065	5.423	12 ± 1	0.0036

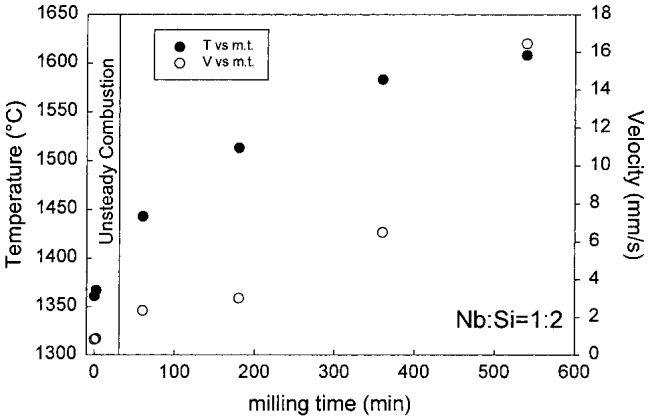

FIG. 2. Dependence of the maximum (peak) temperature (filled symbols) and wave velocity (hollow symbols) on milling time for the composition Nb:Si = 1:2.

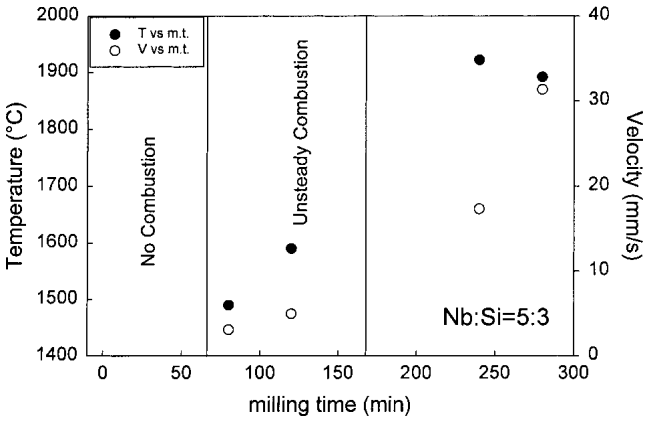

FIG. 3. Dependence of the maximum (peak) temperature (filled symbols) and wave velocity (hollow symbols) on milling time for the composition Nb:Si = 5:3.

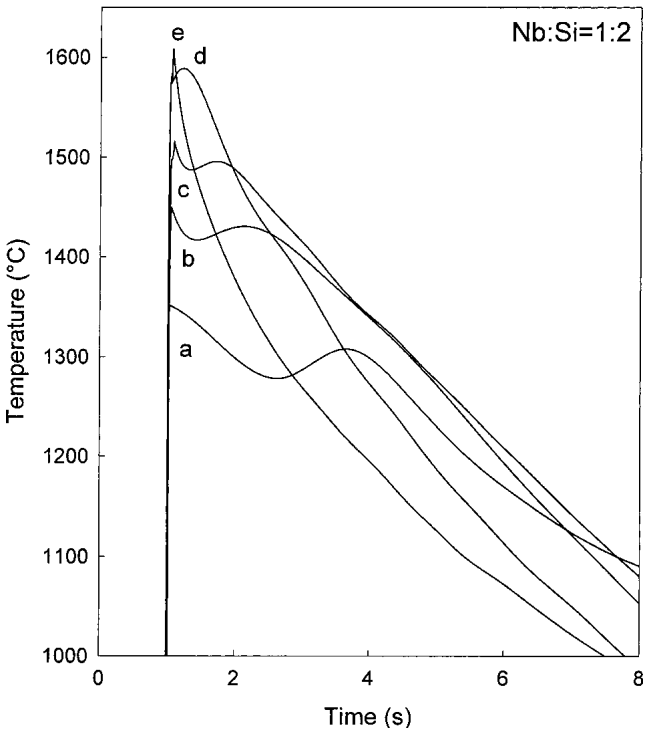

FIG. 4. Temperature profiles for the composition Nb:Si = 1:2, for the following milling times (min): (a) 2; (b) 60; (c) 180; (d) 360; (e) 540.

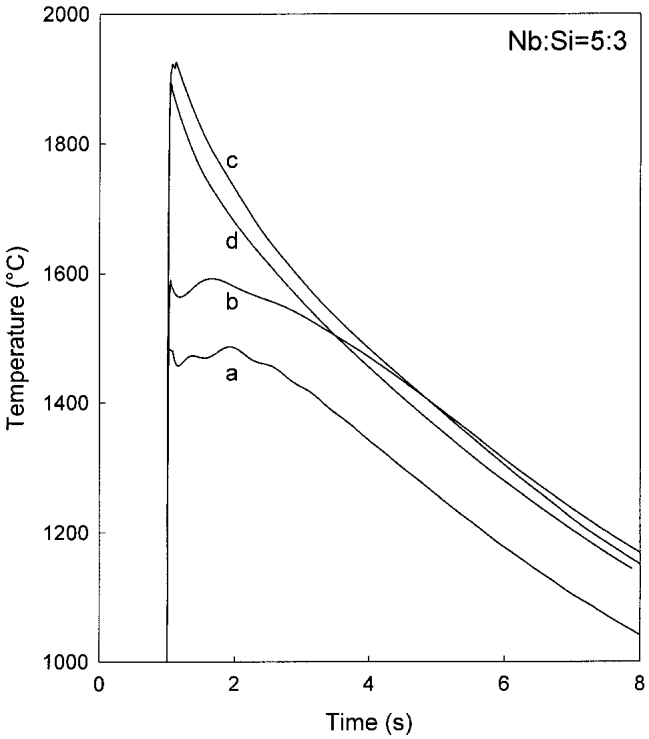

FIG. 5. Temperature profiles for the composition Nb:Si = 5:3, for the following milling times (min): (a) 80; (b) 120; (c) 240; (d) 285.

the spot area (1 mm in diameter) an abrupt increase in temperature is detected. For sake of comparison all the profiles have being aligned as to have the leading edge of the combustion front entering the measure spot at the same time lag (1 s). The temperature profiles at short m.t. appear broader, and a second large peak is present at temperatures slightly lower than the first one. As m.t. is increased, the profile sharpens and the second peak occurs at shorter time lags and finally disappears, giving, for the longest milling times, a very sharp single peak profile. These results suggest that the time required to complete the reaction decreases when finer powders with enlarged surface contact area are employed. This is confirmed in the composition of the products which is presented later.

The final products show a microstructure characterized by a fairly large porosity (65–70%) regardless of m.t. This is a common feature of SHS processes, deriving in part from the original porosity of the green pellet and in part from other sources active during the process itself,[25] like decrease in molar volume, gas evolution due to the expulsion of volatile impurities, and thermal migration resulting from the extremely steep thermal gradients. However, pore size and distribution change considerably with m.t. As can be observed in Fig. 6(a) at low milling times, the pores appear smaller and more uniformly distributed. For long milling times [Fig. 6(b)],

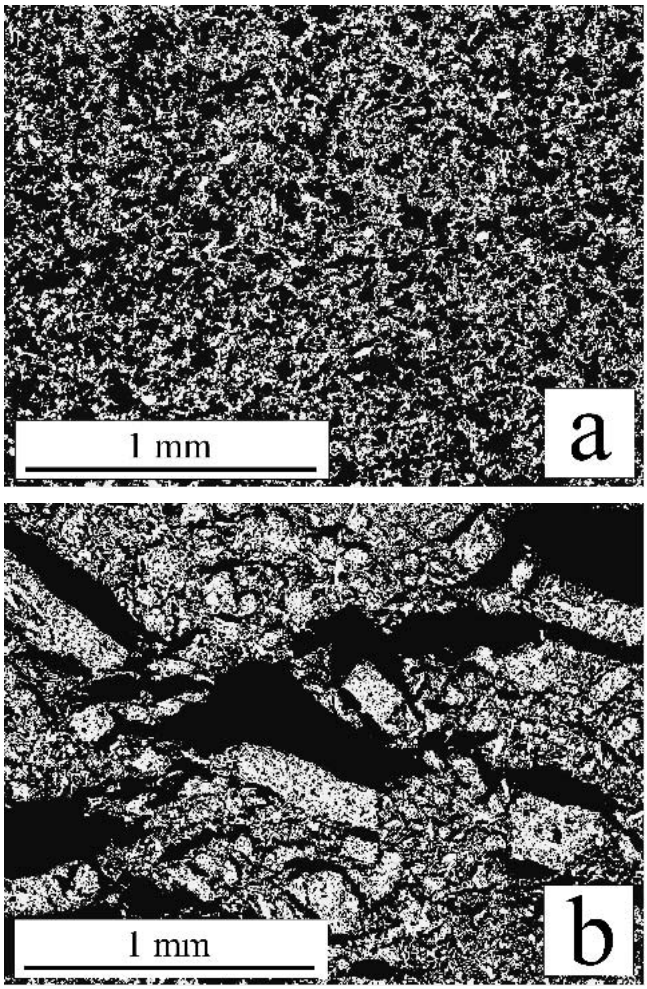

FIG. 6. Microstructure of the end product corresponding to the starting composition Nb:Si = 1:2: (a) m.t. = 2; (b) m.t. = 360 min. The SEM backscattered image is on the polished section.

the products preserve the microstructure characterized by large compact blocks already present in the reacting powders and developed during the milling process.

The composition of the reaction products and the relative amounts (Table III) were evaluated by Rietveld refinement analysis[26,27] of the relevant x-ray diffraction data. In agreement with literature, the composition Nb:Si = 1:2 produced, whatever the m.t., $NbSi_2$ plus traces of the reactants whose quantity decreases with the increase in the milling time. At the longest m.t., a small amount of Nb_5Si_3 appears in the products, probably because of Si losses due to evaporation.

The composition Nb:Si = 5:3 gave, at short milling times, products characterized by a large amount of unreacted Nb and $NbSi_2$. The scarce conversion degree is the obvious main reason for the low tendency, showed by this composition, to sustain the combustion wave. The amount of Nb and $NbSi_2$ in final products decreases considerably at m.t. equal to 2 h, and both disappear completely in the samples characterized by the two longest

m.t. All three crystallographic forms of Nb_5Si_3 have been found including the one usually referred as "carbon stabilized", (hereafter C-Nb_5Si_3). This phase, however, can also be stress stabilized, which is likely to occur in this case, due to the rapid cooling experienced by SHS samples. However, increasing the milling time increases the amount of the β–Nb_5Si_3 and of the "carbon-stabilized" form with respect to the α–Nb_5Si_3 one.

The SEM analysis of the samples characterized by the shortest m.t. which underwent spontaneous interruption of the wave propagation allowed observation of the phase evolution accompanying the wave propagation and hence of the reaction mechanism. Figure 7 shows a SEM image of the zone across the extinct front for a sample of composition Nb:Si = 1:2 (m.t. = 2 min). The arrow indicates the direction of propagation of the combustion front. The sharp change in the microstructure corresponds to the position where the front extinguished (dotted line). In the region ahead of the front limit, only grains of the reactants can be discerned and no indication of any product formation can be detected. At the front position, the dark Si grains disappear due to their melting. The molten Si spreads around the Nb grains leading to the formation of $NbSi_2$. A part of the product surrounds the residual Nb grains, while most of it is present in the form of small precipitates. It must be noted that, at least for this short m.t., the reaction is not complete at the front but a considerable amount of Nb, in the form of the larger grains core, is present well behind the front zone. This is in agreement with the broad temperature profiles previously shown.

TABLE III. Effect of milling on product composition.

Milling time (min)	Product composition (%)					
	$NbSi_2$	Nb	Si	α–Nb_5Si_3	β–Nb_5Si_3	C-Nb_5Si_3
			Nb:Si = 1:2			
0	97.76	0.75	1.48	0	0	0
60	99.91	0.088	0	0	0	0
180	99.79	0.203	0	0	0	0
360	99.77	0.25	0	0	0	0
540	94.35	0.163	0	0.463	0.16	4.85
			Nb:Si = 5:3			
0	35.02	32.6	1.47	25.82	2.81	2.25
80	15.89	18.06	8.87E – 4	41.03	13.89	11.1
120	0	0	0	75.41	13.56	11.02
240	0	0	0	72.97	9.32	17.7
285	0	0	0	48.06	23.34	28.58

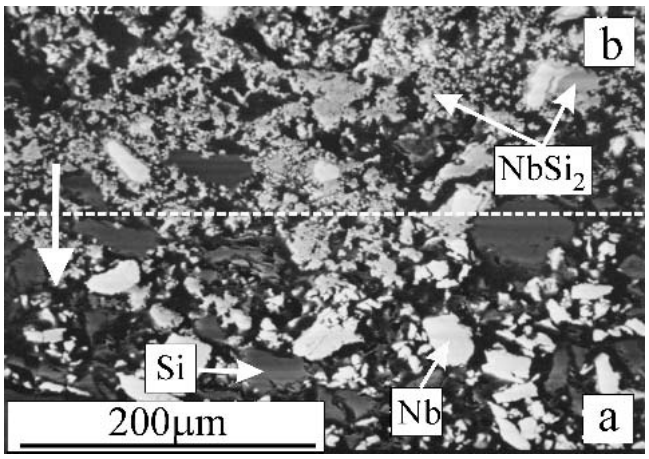

FIG. 7. Spatial evolution of the microstructure during the formation of $NbSi_2$: zone a, reactants; zone b, products. The dotted line indicates the position of the extinguished front. The SEM backscattered image is on the polished section.

B. Diffusion couples

The solid-state diffusion couple experiments showed that the interaction between Nb and Si always produces a double-layer product, as can be seen in Fig. 8. At the Si-rich side, $NbSi_2$ is formed. This phase was always the most conspicuous, and its thickness increases parabolically with time.[24] At the Nb-rich side, a thin Nb_5Si_3 layer is formed. Also Nb_5Si_3 grows parabolically with an integrated diffusion coefficient of more than 1 order of magnitude smaller than the $NbSi_2$ one in the explored temperature range (1200–1350 °C). Figure 9 shows the microstructure resulting from the interaction between Nb and Si when the temperature is above the melting point of Si. The product is similar to the one obtained in solid-solid diffusion couples but with one major difference. The $NbSi_2$ layer appears to be made out of crystals dispersed inside the silicon matrix. However, the dissolution kinetics obtained from these solid–liquid experiments is very different from the one observed with other silicides.[13,28–30] In this case, in fact, the diffusion of Nb in Si liquid appears to be extremely slow. A detailed description of the isothermal reactivity between Nb and Si is reported elsewhere.[24]

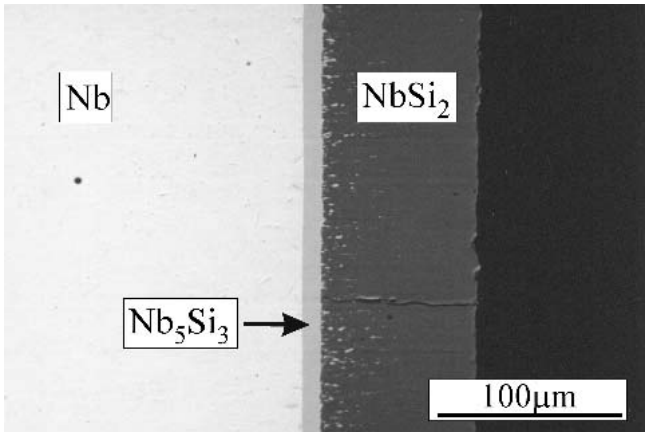

FIG. 8. Backscattered SEM image of a Nb–Si diffusion couple. T = 1350 °C, and t = 16 h. The SEM backscattered image is on the polished section.

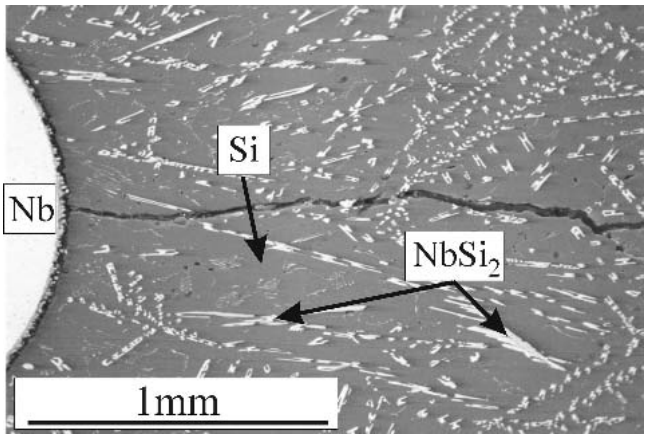

FIG. 9. Microstructure of the product obtained from solid Nb and liquid Si isothermal reaction. $T = 1600$ °C, and $t = 2.5$ min. The SEM backscattered image is on the polished section.

IV. DISCUSSION

The main result of this work is represented by the demonstrated possibility to obtain both $NbSi_2$ and Nb_5Si_3 through combustion processes when mechanical activation of the reactant powders is used. It is worth remembering that the synthesis through combustion of both phases resulted to be problematic using classical SHS, and none of the two silicides could be obtained without preheating, despite the relatively large heat of formation associated with these compounds. Mechanical activation showed a significant influence on both combustion front temperature and propagation rate. Moreover, at sufficiently long m.t., the end products are almost completely free of secondary phases, while it was impossible to obtain pure products using classical SHS coupled with a preheating of reactants.[8] Gedevanishvili and Munir[9] obtained pure Nb_5Si_3 using the FACS method, but any attempt to obtain $NbSi_2$ was unsuccessful due to the poor electrical conductivity of the reacting mixture.

Many of the experimental results reported in this study can be interpreted on the basis of the characteristic of the Nb–Si phase diagram and of the behavior shown by this system when isothermal experiments of reactive diffusion below and above the Si melting point are performed. On this basis, a coherent microscopic mechanism can be suggested.

As observed in Fig. 7 the formation of $NbSi_2$ at the leading edge of the reaction front is due to a dissolution precipitation process.[31] This mechanism has been already recognized to be responsible for the formation of many other MSi_2 phases in the combustion regime ($ZrSi_2$,[28] $CrSi_2$,[29] VSi_2,[30] $TiSi_2$,[13,31] and $TaSi_2$[32]). In this process, following the melting of silicon, the $NbSi_2$ phase forms as a result of the Nb dissolution in melted Si similar to that observed in isothermal experiments of interaction between Nb and melted Si (Fig. 9). However, since the Nb solubility in melted Si is limited (at 1800 °C is only of 15 mol%), the precipitation of the $NbSi_2$ phase starts in the early stages of the interaction. The limited solubility of Nb solid in Si liquid plays an important role in reducing the reactivity and in hindering the combustion reaction in this system. In this regard, two main effects must be considered. First of all, the limited solubility reduces the rate of Nb dissolution in Si. As shown in detail elsewhere,[24] the kinetics of the dissolution process of refractory transition metals in liquid silicon depends strongly on their solubilities at temperatures in the range 1400–1650 °C. Second, and more importantly, it must be remembered that both $NbSi_2$ and Nb_5Si_3 melting points are far higher than combustion temperatures observed in our experiments and once produced they can only be present as solid phases. This requires that the much slower solid state reactivity must be involved to sustain the combustion process. This feature is much more relevant in the case of the composition Nb:Si = 5:3, where the small amount of Si liquid present at the combustion leading edge is rapidly converted into solid $NbSi_2$ representing the primary product of the interaction between Nb solid and Si liquid. Any further advancement of the combustion process requires, per force, the slow solid-state reaction between the primarily formed $NbSi_2$ and the residual Nb to obtain any further advancement of the reaction. This explains the well-known difficulty of obtaining this phase through combustion, despite its considerable heat of formation. A similar situation is observed in the Ta–Si system.[32] This is in contrast with other M–Si systems like Ti–Si, Cr–Si, V–Si, Zr–Si, etc., for which a very efficient dissolution–precipitation process is observed.[17,27–30] The dissolution process is favored by the large solubility of the corresponding transition metals in melted Si (in all these three systems at 1800 °C complete solubility between the metal and silicon is reported)[21] and by the relatively lower melting point of some phases present in these systems. A typical example is represented by the process that leads to the formation of Ti_5Si_3. Despite the fact that the pertinent adiabatic temperatures are similar to the ones involved in the formation of Nb silicides, the reaction between Ti and Si generates combustion waves that are stable and extremely fast even when unmilled powders are used. If we compare the phase diagrams of the two systems, we can observe that not only the solubility of Ti in Si is higher but also the melting point of the primary formed $TiSi_2$ is lower than the measured combustion temperatures. As a result, no solid products are present at the combustion front and appear only in regions behind the front limit.

Within this framework, the mechanical activation step plays a fundamental role in increasing the surface contact area of the powders and decreasing the critical diffusional lengths required for completion of the solid-state reaction, thereby enhancing the overall reactivity of the Nb–Si system. The effects become apparent when one considers the dependence of the combustion temperature

and of the front velocity on milling time. In Figs. 2 and 3, a temperature rise of several hundreds degrees is marked together with an increase of more than 1 order of magnitude in the wave velocity. The rising course of the maximum combustion temperature relates to an intensified and faster release of the reaction heat, as clearly indicated by the sequence of temperature profiles depicted in Fig. 5. Progress in m.t. produces sharper temperature traces, the heat release ending in shorter times as a result of the more rapid microkinetics. Furthermore, the increase in the heat release produces a higher peak temperature due to the heat evolution being faster than the dissipation by conduction at the reaction front. Beside that, microstructure refinement produces higher degrees of chemical conversion at the front leading edge, also increasing the amount of heat release.

A confirmation of the critical role played by particle size on the stability of the combustion front can be found in the literature relative to the combustion behavior of thin multilayers. In fact, it has been reported that layered systems obtained by vacuum or sputter deposition are able to produce self-propagating combustion processes, whose characteristics depend strongly on layer thicknesses.[33] Recently, Reiss *et al.*[34] have shown, as in the case of the Nb–Si system, multilayers can produce combustion reaction characterized by very high propagation rates ($1–4\ m\ s^{-1}$) for layer thickness in the range of tenths of nanometers. A fourfold increase in propagation rate has been observed when the thickness of each bilayer decrease from 310 to 50 nm, due to the decrease in diffusion path required for the reaction. The same mechanism can be considered responsible for the behavior in milled samples as discussed previously, although the much more complex microstructure does not allow a direct quantitative comparison.

V. SUMMARY

Previously reported investigations on the synthesis of niobium silicides by SHS have shown that, despite the high reaction heats involved, a self-sustaining process can be initiated only by preheating the reactants or applying an electric field, the latter method being limited to the Nb:Si = 5:3 composition. Only the field activation leads to a product with uniform composition, while by preheating the reactants, multiphase products were obtained.

In this work, the reactivity in the system Nb–Si was investigated as a function of milling. By prolonged milling of the reactants' mixtures, a self-propagating combustion reaction could be initiated for both compositions without the need of preheating. Moreover, pure products were obtained for both compositions when sufficiently long milling treatments were employed. The enhancement of the reactivity in the Nb–Si system was shown to be determined by the increased surface contact area of the powders and the decreased critical diffusional lengths required for completion of the reaction. Such an effect plays a fundamental role in the Nb–Si reactivity due to the slow kinetics of interdiffusion between the solid elements and the slow dissolution kinetics of niobium into melted silicon.

REFERENCES

1. J.D. Rigney, P.M. Singh, and J.J. Lewandowski, J. Organomet. Chem. **36,** 36 (1992).
2. M.G. Mendiratta and D.M. Dimiduk, in *High-temperature ordered intermetallic alloys III,* edited by C.T. Lui, A.I. Taub, N.S. Stoloff, and C.C. Koch (Mater. Res. Soc. Symp. Proc. **133,** Pittsburgh, PA, 1989), p. 441.
3. M.G. Mendiratta and D.M. Dimiduk, Scr. Metall. **25,** 237 (1991).
4. J.J. Lewandowski, D.M. Dimiduk, W.R. Kerr, and M.G. Mendiratta, in *High-temperature/high-performance composites,* edited by F.D. Lemkey, A.G. Evans, S.G. Fishman, and J.R. Strife (Mater. Res. Soc. Symp. Proc. **120,** Pittsburgh, PA, 1990), p. 103.
5. M.G. Mendiratta, J.J. Lewandowski, and D.M. Dimiduk, Metall. Trans. A **22A,** 1537 (1991).
6. T. Lou, G. Fan, B. Ding, and Z. Hu, J. Mater. Res. **12,** 1172 (1997).
7. B.K. Yen, T. Aizawa, J. Kihara, and N. Sakakibara, Mater. Sci. Eng. **A239–240,** 515 (1997).
8. A.R. Sarkisyan, S.K. Dolukhanyan, and I.P. Borovinskaya, Combust. Explos. Shock Waves **15,** 95 (1979).
9. S. Gedevanishvili and Z.A. Munir, Mater. Sci. Eng. **A211,** 1 (1996).
10. A. Feng and Z.A. Munir, J. Am. Ceram. Soc. **80,** 1222 (1997).
11. B.K. Yen, T. Aizawa, and J. Kihara, J. Am. Ceram. Soc. **81,** 1953 (1998).
12. F. Bernard, F. Charlot, E. Gaffet, and J.C. Niepce, Int. J. Self-Propag. High-Temp. Synth. **7,** 253 (1998).
13. F. Maglia, U. Anselmi-Tamburini, G. Cocco, M. Monagheddu, N. Bertolino, and Z.A. Munir, J. Mater. Res. **16,** 1074 (2001).
14. Ch. Gras, D. Vrel, E. Gaffet, and F. Bernard, J. Alloys Compd. **314,** 240 (2001).
15. G.B. Schaffer and P.G. McCormick, Scr. Metall. **23,** 835 (1989).
16. M. Atzmon, Phys. Rev. Lett. **64,** 487 (1990).
17. A.A. Popovich, V.P. Reva, V.N. Vasilenko, and O.A. Belous, Mater. Sci. Forum **88–90,** 737 (1992).
18. E. Ma, J. Pagan, G. Cranford, and M. Atzmon, J. Mater. Res. **8,** 1836 (1993).
19. L. Takacs, J. Solid State Chem. **125,** 75 (1996).
20. L. Takacs, Mater. Sci. Forum **269–272,** 513 (1998).
21. S. Doppiu, M. Monagheddu, G. Cocco, F. Maglia, N. Bertolino, U. Anselmi-Tamburini, and Z.A. Munir, J. Mater. Res. **16,** 1266 (2001).
22. M.E. Schlesinger, Chem. Rev. **90,** 607 (1990).
23. F. Delogu, L. Schiffini, and G. Cocco, Philos. Mag. A **81,** 1917 (2001).
24. C. Milanese, Ph.D. Thesis, University of Pavia (2001).
25. Z.A. Munir, J. Mater. Synth. Process. **1,** 387 (1993).
26. L. Lutterotti, R. Ceccato, R. Dal Maschio, and E. Pagani, Mater. Sci. Forum **87,** 278 (1998).
27. H.M. Rietveld, J. Appl. Crystallogr. **2,** 65 (1969).
28. N. Bertolino, U. Anselmi-Tamburini, F. Maglia, G. Spinolo, and Z.A. Munir, J. Alloys Compd. **288,** 238 (1999).
29. F. Maglia, U. Anselmi-Tamburini, N. Bertolino, C. Milanese, and Z.A. Munir, J. Mater. Res. **15,** 1098 (2000).
30. F. Maglia, U. Anselmi-Tamburini, C. Milanese, N. Bertolino, and Z.A. Munir, J. Alloys Compd. **319,** 108 (2001).
31. A.S. Rogachev, V.A. Shugaev, I.O. Khomenko, A. Varma, and C.R. Kachelmyer, Combust. Sci. Technol. **109,** 53 (1995).
32. F. Maglia, U. Anselmi-Tamburini, N. Bertolino, C. Milanese, and Z.A. Munir, J. Mater. Res. **16,** 535 (2001).
33. T.S. Dyer, Z.A. Munir, and V. Ruth, Scr. Mater. **30,** 1281 (1994).
34. M.E. Reiss, C.M. Esber, D. Van Heerden, and T.P. Weihs, Mater. Sci. Eng. **A261,** 217 (1999).